Research Article

Ag Doped ZnO Thin Films Synthesized by Spray Coating Technique for Methylene Blue Photodegradation under UV Irradiation

Heri Sutanto,[1] Singgih Wibowo,[1] Iis Nurhasanah,[1] Eko Hidayanto,[1] and H. Hadiyanto[2]

[1]*Department of Physics, Diponegoro University, Jalan Prof. Soedarto, SH, Tembalang, Semarang 50275, Indonesia*
[2]*Department of Chemical Engineering, Diponegoro University, Jalan Prof. Soedarto, SH, Tembalang, Semarang 50275, Indonesia*

Correspondence should be addressed to Heri Sutanto; herisutanto@undip.ac.id

Silver (Ag) substituted ZnO thin films were successfully deposited onto glass substrates by spray coating technique. Structure, morphology, and optical properties were evaluated by X-ray diffractometer (XRD), scanning electron microscopy (SEM), and UV-Vis spectrophotometer, respectively. XRD spectra had polycrystalline wurtzite structure; SEM images showed that thin films had different surface morphology at different Ag doping concentration. From transmittance spectra, thin films transparency decreased as well as band gap energy along with increase of Ag doping concentration. Methylene blue (MB) solution was used as a pollutant in the photodegradation studies. Under UV light irradiation, the optimal Ag doping is 25%, with 83% of the decolorizing efficiencies after 3 h irradiation time and apparent constant (k_{app}) about 9.69×10^{-3} min^{-1}.

1. Introduction

Indonesia has high number of textile industries which usually emit effluents directly into the environment. The effluents contain dyes, oils, and other chemical substances that are so harmful to the environment. The current treatment of textile industrial waste water requires high amount of chemicals and longer treatment time. Therefore an advance technology for treating waste water before being discharge into the environment is required. One of the technologies is by using a photocatalytic treatment to decompose organic pollutants including dyes and other harmless compounds like CO_2 and H_2O [1]. One of the semiconductors that now gain the attention of researchers as a photocatalyst materials is Zinc oxide (ZnO) [2].

ZnO is a direct band gap semiconductor and is found to be useful in various applications such as photocatalysts, electronics, and cosmetics [1]. However, for photocatalytic application, it is desirable that ZnO should absorb not only UV but also visible light due to the fact that visible light accounts for 45% of energy in the solar radiation, while UV light accounts for less than 10%. Addition of cations

(transition metals) and anions (nitrogen, sulfur, carbon, or boron) into the semiconductor has been extensively studied to enhance the activity of photocatalyst [3, 4].

Addition of metal into ZnO using appropriate dopant and method can improve their applications performance. As an example in the photocatalytic application, ZnO can be added with Ag elements to improve efficiency. The Ag ions can act as acceptors in ZnO and may change Zn ions. Moreover, the addition of Ag ions can also reduce the energy gap in semiconductors so it can increase the absorption of light wavelength [5–7].

There are various methods that can be used to create a ZnO thin film such as pulsed laser deposition (PLD) [8], spray pyrolysis [9], metal oxide chemical vapor deposition (MOCVD) [10], and sol gel [11]. Sol gel is one of the most widely used methods because it is easy to prepare and of low cost. In this study, we made Ag substituted ZnO thin films by sol gel method. In order to test the photocatalytic activity, we used methylene blue (MB) as a pollutant and photodegradation conducted for 3 h under UV light irradiation. The objective of this paper is to evaluate the substitution high

concentration Ag into ZnO and to evaluate its application for methylene blue (MB) degradation.

2. Experiment

Ag substituted ZnO (Ag-ZnO) thin films were prepared by using sol gel spray coating technique onto glass substrates. Zinc acetate $Zn(CH_3COO)_2 \cdot 2H_2O$ (Merck, 99.5%) and silver acetate (CH_3COOAg) (Sigma Aldrich, 99%) were used as ZnO and Ag source, respectively. Prior to using glass substrates for Ag-ZnO deposition, they were cleaned with acetone, methanol, and deionized water. An appropriate quantity of silver acetate powder was dropped into the zinc acetate solution to accomplish different doping concentration (i.e., 0 mol%, 5 mol%, 10 mol%, 15 mol%, 20 mol%, and 25 mol%) and subsequently the initial and deposited samples are denoted by ZA5, ZA10, ZA15, ZA20, and ZA25, respectively.

The structural and morphological characterizations were carried out using Shimadzu Maxima 7000 X-ray diffractometer with CuKα radiation (1.5405 Å) and scanning electron microscopy (SEM) JEOL-JSM 6510 LA, respectively. The optical study was carried out using UV-Vis spectrophotometer (Shimadzu 1240 SA).

The photocatalytic test was performed in an aqueous solution using methylene blue ($\lambda = 664$ nm) as the probe molecule. The samples were irradiated with UV (A) light (10 W UV tube, Aquaco). The Ag-ZnO films were horizontally fixed in the middle of beaker. The dye solution (40 mL) and samples were irradiated with light source placed horizontally above the beaker. The photodegradation of the dye was followed by measuring the absorption spectra at regular interval (every 30 min) using a UV-Vis spectrophotometer (Shimadzu 1240 SA).

MB degradation efficiency (η) was calculated according to

$$\eta = \frac{(C_0 - C)}{C_0} \times 100, \tag{1}$$

where C_0 represents the initial concentration and C represents the concentration after t minutes of photocatalysis.

3. Results and Discussion

3.1. X-Ray Diffractogram (XRD) Analysis. The changes in the structure and phase identification of Ag-ZnO thin films were conducted by XRD analysis. The diffracting angle (2θ) was varied between 10° and 90° and the spectra were recorded for all the samples which are shown in Figure 1. All the films show polycrystalline with mixed phases of Ag and ZnO. The diffraction peaks corresponding to ZnO and Ag are in good agreement with standard JCPDS data card #36-1451 and #45-1027, respectively. The diffraction peaks at (2θ) 31.76°, 34.42°, 36.24°, and 56.60° are corresponding to hexagonal wurtzite ZnO phase with plane (100), (002), (101), and (110), respectively, while the diffraction peaks at 38.16° and 44.40° are related to the Ag phase with planes (111) and (200), respectively.
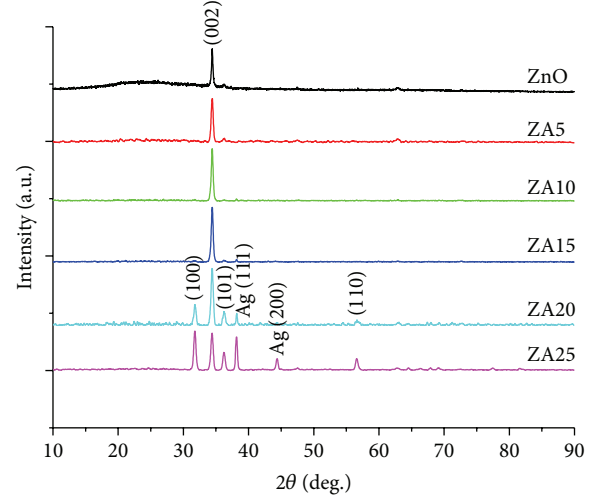

FIGURE 1: X-ray pattern of Ag-ZnO thin films prepared by thermal spray coating at 450°C.

TABLE 1: Different interplanar spacing d_{hkl} of Ag-ZnO sprayed thin films.

	d_{002} (Å)	d_{101} (Å)	c (Å)
ZnO	2.6019	2.4780	5.2039
ZA5	2.6034	2.4768	5.2067
ZA10	2.6032	2.4761	5.2064
ZA15	2.6031	2.4745	5.2061
ZA20	2.6037	2.4756	5.2073
ZA25	2.6050	2.4768	5.2101

The interplanar spacing d_{hkl} values of given Miller indices h, k, and l of Ag doped ZnO thin films were also calculated by using Bragg equation as follows [12]:

$$2d_{hkl} \sin \theta = n\lambda, \tag{2}$$

where n is the order of diffraction (usually $n = 1$) and λ is the X-ray wavelength. The plane spacing is related to the lattice constants a, c and the Miller indices in ZnO hexagonal structure by the following equation [12]:

$$\frac{1}{d_{hkl}^2} = \frac{4}{3} \left(\frac{h^2 + hk + k^2}{a^2} \right) + \frac{l^2}{c^2}. \tag{3}$$

Both lattice parameters a and c for the hexagonal closed-packed (HCP) are calculated via (002) and (101) orientations [12]. Table 1 summarizes also the calculated values of interplanar spacing d_{hkl} of Ag doped ZnO thin films.

It can be seen from the results that the value of c in the ZnO layer is greater than the standard value of c_o ZnO powder (0.5205 nm) [13]. Increasing value of c is caused by a radius of Ag^+ (1.26 Å) which is greater than Zn^{2+} (0.74 Å) when Ag is on the Zn site [13]. An increase in the lattice parameter can be also caused by interstitial incorporation of Ag ions into the lattice or Ag ion substitution of the Zn ions [13].
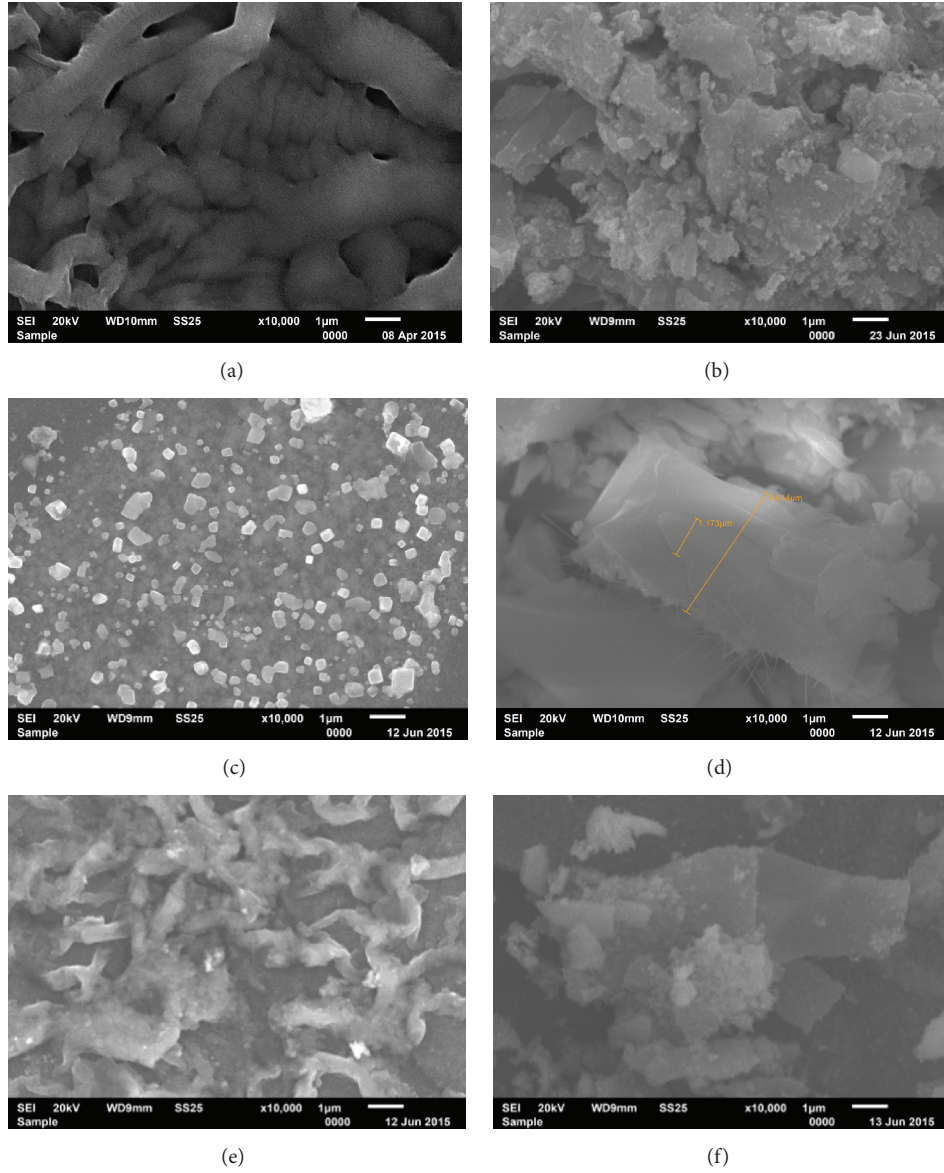
(a)

(b)

(c)

(d)

(e)

(f)

FIGURE 2: SEM images of (a) ZnO, (b) ZA5, (c) ZA10, (d) ZA15, (e) ZA20, and (f) ZA25.

TABLE 2: FWHM and grain size of Ag-ZnO sprayed thin films.

	2θ	FWHM (θ)	D (nm)
ZnO	34.4127	0.3305	24.7472
ZA5	34.4204	0.3720	21.9845
ZA10	34.4224	0.3579	22.8564
ZA15	34.4245	0.3644	22.4475
ZA20	34.4165	0.4159	19.6658
ZA25	34.3977	0.4219	19.3861

Table 2 depicts the grain size D values that were estimated from (002) diffraction lines of ZnO free and Ag doped ZnO thin films using Scherrer formula [12]:

$$D = \frac{k\lambda}{\beta_{1/2} \cos\theta}, \qquad (4)$$

where $k = 0.90$ is Scherrer constant, $\beta_{1/2}$ is the width at half-maximum, and $\lambda = 1.54$ Å is the wavelength of CuKα radiation.

3.2. Scanning Electron Microscopy (SEM) Analysis. The surface morphological study of the synthesized thin films was carried out using scanning electron microscopy (SEM). Figures 2(a)–2(f) show the SEM images with ×10.000 magnification of all samples deposited at 450°C onto glass substrates. SEM images reveal that the films surface are different in each Ag concentration. At ZnO we found that the surface has thread-like morphology. ZA5 morphology does not have uniform surface, while in ZA10 a lot of particles in uniform size are clearly shown. ZA15 shows that the film has nonuniform surface. Thread-like morphology is shown in ZA20. The same result was observed by Tarwal and Patil [14]. At ZA25, the film surface is not uniform just like ZA5 and ZA15. Shidpour
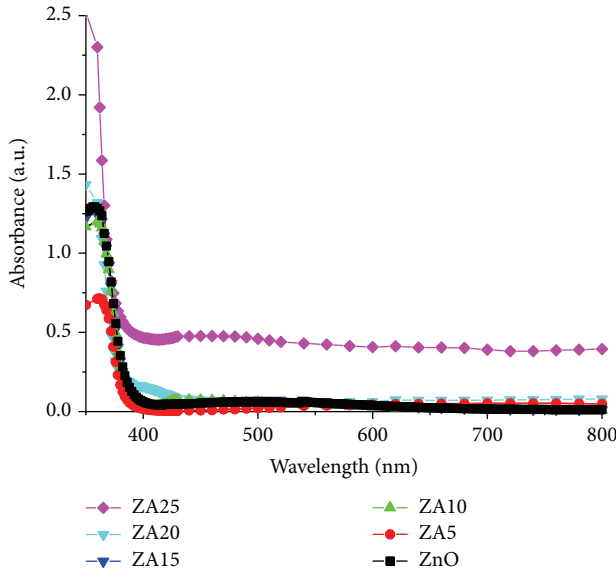
FIGURE 3: UV-Vis absorption spectra of Ag-ZnO thin films.

FIGURE 4: Transmittance spectra of Ag doped ZnO thin films.

et al. [15] showed that the different surface morphology determined the outcome of photocatalytic activity, which is indicated by nanowire-like morphology as having higher photocatalytic activity than nanoporous.

3.3. UV-Vis Spectrophotometer Analysis. Figure 3 shows the absorbance spectra as a function of wavelength for Ag-ZnO thin films deposited on glass substrates prepared by sol gel spray coating. It can be seen that increase of Ag concentrations makes slightly shifts of absorption edge to higher wavelengths. In addition, the nearly flat spectra are shown in the higher wavelength area. This is due to the larger amount of Ag, increasing the substitution of Zn ion by Ag ions.

Figure 4 shows the transmittance spectra for Ag-ZnO thin films. The transmittance spectra are formed by interference of light at the interface between the films and the substrate. Transmittance spectra of Ag-ZnO films in the visible region decrease from 90 to 30% as the Ag percentage increases. This decrease in the transmittance value of the Ag-ZnO thin films may be due to the grain boundary scattering. It is also caused by surface plasmon resonance (SPR) related phenomenon of Ag nanoparticles which can absorb the visible light.

Absorption coefficient and band gap for the direct band gap semiconductor obey the following relationship:

$$(\alpha h\nu)^2 = A\left(h\nu - E_g\right), \tag{5}$$

where α is the absorption coefficient, $h\nu$ is the photon energy, A is a constant, and E_g is the optical band gap. The optical band gap E_g can be obtained by extrapolating the linear part of the curve to $(\alpha h\nu)^2 = 0$ if one plots $(h\nu)^2 \sim h\nu$. The related curves for our samples are shown in Figure 5. The optical band gap energy for Ag-ZnO thin films is found to be in the range of 2.98 eV to 3.12 eV. The band gap narrowed with
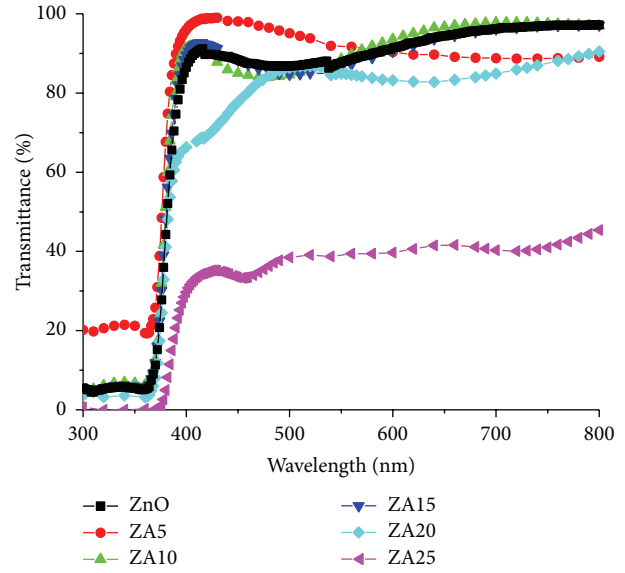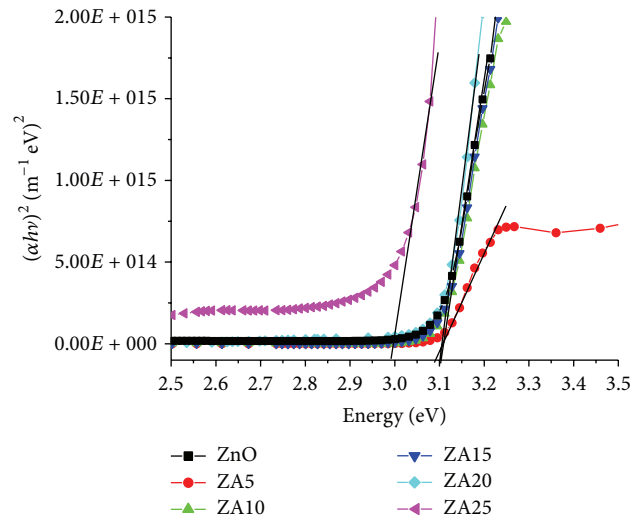

FIGURE 5: Optical band gap of Ag-ZnO thin films.

increasing Ag contents. It means that Ag^+ was substituted into Zn^{2+} [13].

3.4. Photocatalytic Study. The photocatalytic process occurs when the ZnO material is irradiated by light that its energy is greater than the gap energy of ZnO. Electrons (e^-) and holes (h^+) are formed in the conduction band and valence band, respectively. Then, holes will react with water to form OH^*, while the electrons form superoxide (O_2^{*-}) and subsequently form other reactive oxygen species (H_2O_2 and OH^*).

Holes and OH^* are highly reactive toward organic pollutants if they are in contact. The C-C and C-H bonds of MB adsorbed on the surface of Ag-ZnO thin films can be destroyed by the oxidizing power of OH^* radicals leading to CO_2 and H_2O production [16]. Thin films were immersed in 40 mL MB (10 ppm) and irradiated with UV (A) for 3 h.
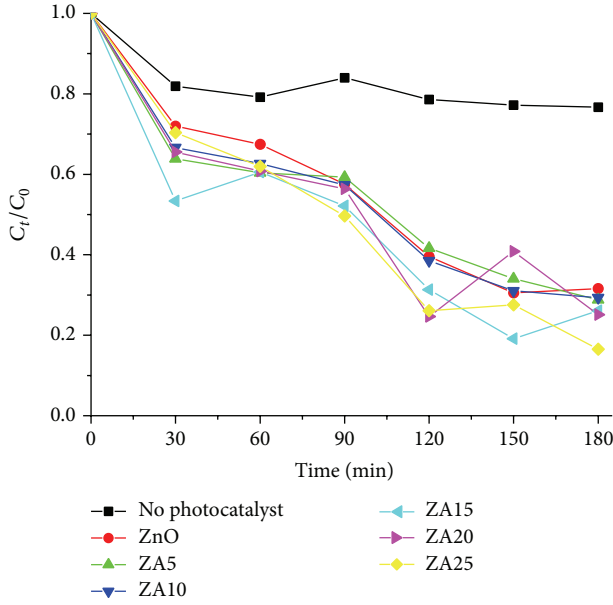
FIGURE 6: Degradation under UV irradiation with various films.

TABLE 3: Apparent rate constants of methylene blue degradations.

Thin films	$k_{app} \times 10^{-3}$ (min^{-1})	R^2
ZnO	6.79	0.95
ZA5	6.38	0.94
ZA10	6.78	0.95
ZA15	8.02	0.81
ZA20	7.14	0.76
ZA25	9.69	0.95
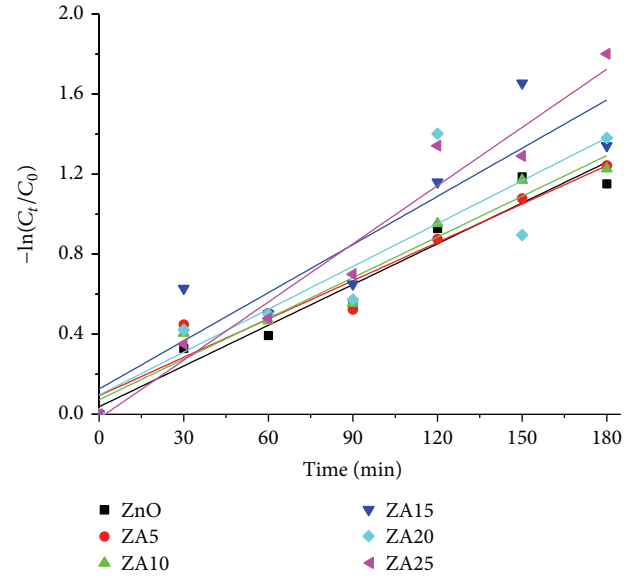
FIGURE 7: Kinetic degradation of MB under UV irradiation with various films.

The photodegradation of the MB under UV (A) light irradiation was determined by measuring absorption spectra using UV/Vis spectrophotometer. Figure 6 shows the relationship between difference of concentration (C_t/C_0) and irradiation time.

It can be seen that the photocatalytic degradation of MB by Ag-ZnO thin films is up to 83% after 3 h, while the MB without photocatalyst shows flat line about 18%. This result informs that, without photocatalysts, MB does not significantly change. The addition of Ag on ZnO can improve the photocatalytic activity due to the active hydroxyl radical formation on the surface of ZnO [17]. On the other hand, there was also an influence of surface plasmon resonance (SPR) effect that can increase the photocatalytic activity by the increase of optical absorbance and charge carrier separation under UV irradiation [17].

Langmuir-Hinshelwood model describes the kinetic of photocatalytic degradation of MB and the photocatalytic degradation rate (r) is given by the following equation [16]:

$$r = -\frac{dC}{dt} = \frac{k_r K_{dye} C}{1 + K_{dye} C}, \tag{6}$$

where dC/dt is the degradation rate (mgL^{-1}min^{-1}), C is the dye concentration (mgL^{-1}) at the irradiation time (t), k_r is the rate constant (min^{-1}gL^{-1}), and K_{dye} is the adsorption coefficient of the dye (Lmg^{-1}). Equation (7) is simplified into the first-order kinetic model with an apparent first-order rate constant k_{app} (min^{-1}) and at low concentrations ($K_{dye}C \ll 1$) [16]:

$$\ln\left(\frac{C_t}{C_0}\right) = -k_r K_{dye} t = -k_{app} t. \tag{7}$$

The constants k_{app} of MB are determined from the slopes of the linear plots $\ln(C_t/C_0)$ against the time (t) (Table 3).

Figure 7 shows that ZA25 has highest apparent first-order rate constant (k_{app}) about 9.69×10^{-3} min^{-1} and the correlation coefficient about 0.95. These results are consistent with the results of the band gap ZA25, which is smaller than the other layers. The smaller gaps of energy band will facilitate the electrons movement from the valence to the conduction band, thus increasing the photocatalytic process.

4. Conclusion

Ag-ZnO thin films have been successfully synthesized onto glass substrates by using sol gel spray coating technique. From X-ray diffraction analysis, the films have polycrystalline spectra with wurtzite structure. The SEM images showed different morphology on each Ag doping concentration. The surface morphology for the sample ZnO and ZA20 shows thread-like morphology. Optical properties of Ag-ZnO thin films show that transparency decreases along with increase of Ag content. The absorbance spectra of thin films are slightly shifted to higher wavelengths and ZA25 has lowest energy gap about 2.98 eV. The photocatalytic degradation of MB solution using Ag-ZnO thin films was investigated under UV light irradiation. Sample ZA25 has the highest efficiency on photodegradation of MB.

Conflict of Interests

The authors declare that there is no conflict of interests regarding the publication of this paper.

Acknowledgment

References

[1] G. Poongodi, R. M. Kumar, and R. Jayavel, "Structural, optical and visible light photocatalytic properties of nanocrystalline Nd doped ZnO thin films prepared by spin coating method," *Ceramics International*, vol. 41, no. 3, pp. 4169–4175, 2015.

[2] H. Sutanto, I. Nurhasanah, and E. Hidayanto, "Deposition of Ag 2~6 mol%-doped ZnO photocatalyst thin films by thermal spray coating method for *E. coli* bacteria degradation," *Materials Science Forum*, vol. 827, pp. 3–6, 2015.

[3] S. Anandan, N. Ohashi, and M. Miyauchi, "ZnO-based visible-light photocatalyst: band-gap engineering and multi-electron reduction by co-catalyst," *Applied Catalysis B: Environmental*, vol. 100, no. 3-4, pp. 502–509, 2010.

[4] M. G. Nair, M. Nirmala, K. Rekha, and A. Anukaliani, "Structural, optical, photo catalytic and antibacterial activity of ZnO and Co doped ZnO nanoparticles," *Materials Letters*, vol. 65, no. 12, pp. 1797–1800, 2011.

[5] H. Q. Bian, S. Y. Ma, Z. M. Zhang, J. M. Gao, and H. B. Zhu, "Microstructure and Raman scattering of Ag-doping ZnO films deposited on buffer layers," *Journal of Crystal Growth*, vol. 394, pp. 132–136, 2014.

[6] Y. Zhang, Z. Zhang, B. Lin, Z. Fu, and J. Xu, "Effects of Ag doping on the photoluminescence of ZnO films grown on Si substrates," *The Journal of Physical Chemistry B*, vol. 109, no. 41, pp. 19200–19203, 2005.

[7] J. Fan and R. Freer, "The roles played by Ag and Al dopants in controlling the electricalproperties of ZnO varistors," *Journal of Applied Physics*, vol. 77, no. 9, pp. 4795–4800, 1995.

[8] Q. Li, Y. Wang, J. Liu, W. Kong, and B. Ye, "Structural and magnetic properties in Mn-doped ZnO films prepared by pulsed-laser deposition," *Applied Surface Science*, vol. 289, pp. 42–46, 2014.

[9] S. Vijayalakshmi, S. Venkataraj, M. Subramanian, and R. Jayavel, "Physical properties of Zinc Doped thin oxide films prepared by spray pyrolysis technique," *Journal of Physics D: Applied Physics*, vol. 41, no. 1, pp. 1–7, 2008.

[10] J.-P. Biethan, V. P. Sirkeli, L. Considine, D. D. Nedeoglo, D. Pavlidis, and H. L. Hartnagal, "Photoluminescence study of ZnO nanostructures grown on silicon by MOCVD," *Materials Science and Engineering: B*, vol. 177, no. 8, pp. 594–599, 2012.

[11] H. Sutanto, I. Nurhasanah, and H. Hadiyanto, "Effect of Mn concentration on magnetic and structural properties of GaN:Mn deposited on silicon substrate using chemical solution deposition method," *Romanian Journal of Materials*, vol. 44, no. 3, pp. 298–303, 2014.

[12] M. Karyaoui, A. Mhamdi, H. Kaouach et al., "Some physical investigations on silver-doped ZnO sprayed thin films," *Materials Science in Semiconductor Processing*, vol. 30, pp. 255–262, 2015.

[13] H. Q. Bian, S. Y. Ma, F. M. Li, and H. B. Zhu, "Influence of ZnO buffer layer on microstructure and raman scattering of ZnO:Ag film on Si substrate," *Superlattices and Microstructures*, vol. 58, pp. 171–177, 2013.

[14] N. L. Tarwal and P. S. Patil, "Enhanced photoelectrochemical performance of Ag-ZnO thin films synthesized by spray pyrolysis technique," *Electrochimica Acta*, vol. 56, no. 18, pp. 6510–6516, 2011.

[15] R. Shidpour, A. Simchi, F. Ghanbari, and M. Vossoughi, "Photodegradation of organic dye by zinc oxide nanosystems with special defect structure: effect of the morphology and annealing temperature," *Applied Catalysis A: General*, vol. 472, pp. 198–204, 2014.

[16] S. Boumaza, F. Kaouah, D. Hamane, M. Trari, S. Omeiri, and Z. Bendjama, "Visible light assisted decolorization of azo dyes: direct Red 16 and Direct blue 71 in aqueous solution on the p-$CuFeO_2$/n-ZnO system," *Journal of Molecular Catalysis A: Chemical*, vol. 393, pp. 156–165, 2014.

[17] J. Lu, H. Wang, S. Dong, F. Wang, and Y. Dong, "Effect of Ag shapes and surface compositions on the photocatalytic performance of Ag/ZnO nanorods," *Journal of Alloys and Compounds*, vol. 617, pp. 869–876, 2014.